ACTA METALLURGICA SLOVACA
2021, VOL. 27, NO. 3, 103-108

RESEARCH PAPER

THE EFFECT OF MATERIAL MODELS IN THE FEM SIMULATION ON THE SPRINGBACK PREDICTION OF THE TRIP STEEL

Peter Mulidrán[1)], Emil Spišák[1)], Miroslav Tomáš[1)], Janka Majerníková[1)], Ján Varga[1)]*

[1] Institute of Technology and Material Engineering, Faculty of Mechanical Engineering, Technical University of Košice, Mäsiarska 74, 040 01, Košice, Slovakia

* Corresponding author: peter.mulidran@tuke.sk, tel.: +421556023516, Faculty of Mechanical Engineering, Technical University of Košice, 04001, Košice, Slovakia

Received: 15.03.2021
Accepted: 18.06.2021

ABSTRACT

In this work, the influence of material models used in the FEM simulation on the springback prediction is investigated. The interest of this paper is to extend the knowledge base regarding springback predictions in numerical simulation. The springback effect of a V-shaped sheet metal part made of TRIP steel, with a thickness of 0.75 mm was investigated. The bending angle was set to 90°. In the numerical simulation, Hill48 and Barlat yield criteria were used in combination with Ludwik's and Swift's hardening models. Achieved data from the numerical simulations were compared and evaluated with experimental test results. Also, the effect of bending radius, calibration force, and specimen cut direction on the springback was investigated. The experimental results showed the relation between springback and calibration force. The effect of specimen cut direction on the springback was smaller in comparison with the calibration force. The numerical results of the springback were not identical with the experimentally achieved springback values in most cases. Particularly, when a calibration force of 1 800 N was used in the simulation. The simulation results showed a good correlation between experimental and numerical results, when Hill48 and Barlat yield criteria were used in combination with Ludwik hardening law and calibration force F with the value 900 N was applied.

Keywords: springback, numerical simulation, material models, yield criterion

INTRODUCTION

High-strength steel has been used by automobile manufacturers for almost thirty years now. The main reason for using these types of steels is to increase the passive safety of the vehicles and to reduce the weight of these vehicles. The reduction of weight mainly contributes to higher fuel efficiency. However, high-strength steels have lower formability and greater springback in comparison with conventional steels used for drawing, the main reason for that is the higher value of the yield strength and lower ductility of these steels (**Fig. 1**) [1, 2].

The TRIP steels, or Transformed Induced Plasticity steels, have higher values of mechanical properties (yield strength and tensile strength) if compared with conventional steels [3]. Strain hardening is also greater; therefore they offer a superior combination of strength and formability properties which can be contributed to the multiphase structure of these steels. The main characteristic of TRIP steels is that they modify the microstructure during the plastic deformation process as part of the austenite transformation to martensite, with the following change of the material properties. One of the main issues of TRIP steels is strong elastic recovery, also known as springback, which occurs after forming. [4, 5].

The bending process is one of the most utilized manufacturing technologies and it represents plastic deformation of the material which occurs when the bending moment is applied. Accurate bending of the steel sheets requires at the design stage of the manufacturing process to consider mechanical and other properties of the sheet material, i.e., elasticity modulus, yield stress, ratio of yield stress to ultimate tensile stress, and microstructure of the material [6]. The non-uniform strain state at the section of material that was exposed to bending moment leads to the creation of residual stress after external load removal. The residual stress produces springback which is developed by involuntary changes in the shape of the part after the forming.

The springback can be measured or expressed as springback coefficient or as springback angle [1]. A general countermeasure against springback is to design forming tools that expect springback compensation, but the compensation amount is a difficult matter even for experienced tool designers and manufacturing practice is still largely based on trial and error. Also, it is problematic to use the same forming tool for the forming of different types of materials. The reason for that lays in the different values of mechanical and plastic properties. Specific tolerances have to be made in die design so that the final stamping will fulfill the engineer's objective for both appearance and ease of assembly. Other countermeasures against springback include for example stiffening of stampings (use of beads or embossing), crash forming with pressure pad, or use of variable blank holder force, etc. [7, 8]. Lawanwong et al. [9] proposed a novel technology called “double-action bending” to eliminate the springback of the stamped part made of advanced high-strength steel. They used FE analysis to determine process and tool parameters before the experiment try-out. Also in the industries which produce stampings, such as the automotive industry, accurate predictions of forming process, including stress-strain distribution, springback and thickness are necessary [10]. Today it is feasible to use finite element analysis for a more accurate prediction of the springback effect [11, 12]. The finite element analysis (FEA) is a modern tool that can help to achieve more accurate springback predictions [13, 14]. Several authors conducted experiments and simulations

regarding springback investigation. Mulidrán et al. [15] conducted numerical simulations regarding the springback prediction of aluminum alloy A-pillar. They used various combinations of yield criteria and hardening laws to predict the springback of the part. Neto, D et al. [16] work was focused on the wrinkling and springback prediction. Their research was mainly focused on the influence of applied boundary conditions in simulation. Also, they compared wrinkling tendency between mild-steel DC06 and dual-phase steel DP600. Slota et al. [17] research was focused on the investigation of technological parameters, blank holding force, and friction and their impact on springback in U bending with stretching process. They also used numerical simulation to predict springback. They used the Hill'48 yield criterion in the combination with the hardening curve defined by Hollomon. Seo et al.'s [18] work was focused on the evaluation of the effects of constitutive equations on the springback prediction accuracy. They used two yield functions, Hill48 and Yld2000, in combination with the Yoshida–Uemori hardening model in the FEM simulation to predict the springback effect on the U-bend part and drawn T-shape part. Both parts were made of TRIP steel. Baara et al. [19] worked on the new constitutive hardening material model which can achieve more accurate springback predictions. The main objective of their work was to extend the Chord model to be able to reproduce the strain recovery point with non-zero residual stress, enabling a more accurate determination of springback. Cui et al. [20] proposed a new stamping method for forming the L-shaped part. They call this method electromagnetic-assisted stamping (EMAS). They used a magnetic force to control the springback phenomenon. The results showed that as discharge voltage increases, the bent angle after springback decreases. Mulidrán et al. [21] performed bending experiments and simulations of deep-drawing quality steel. Their work was aimed to study the accuracy of springback prediction. The previously mentioned works were not aimed to study the effects of material models on the springback prediction of V-shaped parts made of TRIP steel. Additionally, the influence of material models on the springback prediction under different process conditions was evaluated to expand the current state of knowledge.

In this study, springback prediction results of the V-shaped part made of hot-dip galvanized TRIP steel RAK 40/70, with a thickness of 0.75 mm were compared with experimental test results. This steel is part of high strength steel group and was chosen for this study, because of its higher yield strength value in comparison with conventional steels. Also, high-strength steels are not included in the standard STN 22 7340:1990-11: Stamping dies. Bending dies. General requirements for calculation and design. This can cause problems for tool designer when high strength steels are used as material for forming/bending. The springback prediction has been conducted with the use of FEA, in the environment of the forming simulation software Autoform. In the FE analysis of forming steel sheets, it is important to input correct process, geometrical, numerical, and material parameters (**Fig. 2**). In this work, two types of yield surface models: The Hill48 model and Barlat model in combination with two hardening models: Swift model and Ludwik model were used for springback prediction using CAE software. Also, effects of bending radius R [mm], calibration force F [N], and specimen cut direction [°] on the springback was evaluated. This work aimed to evaluate the impact of previously mentioned parameters on the stampings´ springback and to examine the influence of the used material models in the numerical simulation.

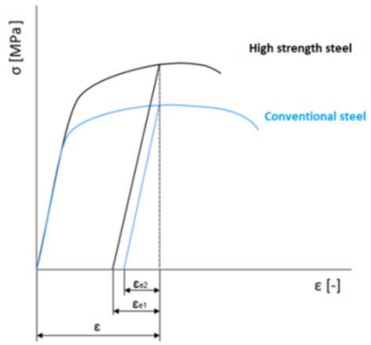

Fig. 1 Stress-Strain curve describing the impact of yield strength on elastic deformation

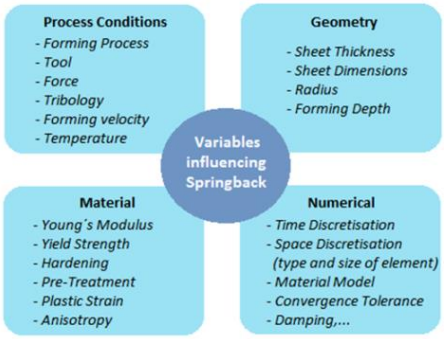

Fig. 2 Variables influencing springback prediction

MATERIAL AND METHODS

Experimental procedure

The experimental testing was conducted in the Laboratory of Testing Mechanical Properties, which is part of the Institute of Technology and Material Engineering. The material properties of the hot-dip galvanized TRIP steel RAK 40/70 are presented in **Table 1**. Testing of material properties was done according to the standards STN EN ISO 6892-1:2019 Metallic materials - Tensile testing - Part 1: Method of test at room temperature, STN EN ISO 10113: 2020 Metallic materials - Sheet and strip - Determination of plastic strain ratio, and STN EN ISO 10275: 2020 Metallic materials - Sheet and strip - Determination of tensile strain hardening exponent. These tests were performed on the material test machine TIRAtest 2300. This test machine is equipped with a tensometer, longitudinal extensometer, and also with a sensor that is used for measuring the width of the tensile test specimen during testing. Tensile test specimens were prepared according to STN EN ISO 6892-1:2019standard. The bending experiments were conducted on hydraulic press ZD-40. This device also consists of a tensometer which was used to measure applied force. The Control unit of ZD-40 collected force data, which were then transferred to PC and later processed in Excel. **Fig. 3** shows a bending tool (left) tool scheme with dimensions (right) for the experimental testing.

The bending angle, angle of working surfaces of a bending tool was 90 degrees. Two punches with different bending radiuses R (R1= 1 mm, R2= 3 mm) were used in testing. The blank used

for bending had a rectangular shape with dimensions of 90 mm x 40 mm. These specimens were cut 0° and 90° to the rolling direction. The thickness of the blank was 0.75 mm. Blanks were prepared using hydraulic shears LVD CS6/31. Three variables, which affect springback were experimentally tested and evaluated:

- bending radius R [mm],
- calibration force F [N],
- specimen cut direction [°].

The calibration force values were determined during experimental testing. The lowest value of 460 N represents bending without calibration. The second value was approximately 2 times the bending force value. The third value of the calibration force 1800 N (app. 4 times the bending force) was chosen. For each variable, five specimens were used in the testing. The impacts of these three variables on the springback are evaluated in the Results and discussion section.

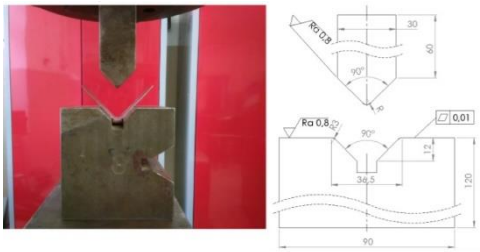

Fig. 3 Experimental tool used for bending (left), tool scheme with dimensions (right)

The springback measurement consisted of measuring arm opening angle ß [°] as shown in **Fig. 4**. The stamping image after bending was imported into AutoCAD and the angle between arms was measured.

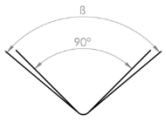

Fig. 4 Measurement of springback angle – arm opening angle ß

Simulation procedure

The numerical simulations of bending TRIP steel sheets were conducted in CAE forming software Autoform R3 which uses a special implicit method and adaptive mesh algorithms. Tool geometry is an important factor in sheet metal forming. Thus it is also important to correctly model forming tools which are then used in CAE software. Imported CAD model of experimental tool, which was used in numerical simulation, is pictured in **Fig. 5**.

The Geometry, dimensions of the CAD model of the tool were the same as in the experimental bending tool. After importing the CAD model into the CAE environment, the tool surfaces needed for simulation were meshed with triangular shell elements. The tools were modeled as rigid bodies. The accuracy of the numerical simulation was set to fine. With this setting, the program automatically generates mesh parameters for blank. Blank also consisted of triangular elements. The Initial element size of the shell element was set to 3 mm with a maximal refinement level of 2. Radius penetration was set to 0.16; a number of integration points was set by software to 11. The maximum time step was set to 0.5 s and the coefficient of friction value was set to 0.27. This value was selected because of the higher friction which occurs between zinc plated steel and tool steel (with no lubrication) compared to friction pair steel-steel [22].

Table 1 Mechanical properties of RAK 40/70 TRIP steel

Direction [°]	**Yield strength σ_y [MPa]**	**Tensile strength σ_u [MPa]**	***Young´s modulus E [GPa]***	***Uniform elongation A_{80} [%]***	***Strain hardening exponent n [-]***	***Coefficient of normal anisotropy r [-]***	***Planar anisotropy coefficient Δr [-]***	***Poisson´s ratio V [-]***
0	441	766	210	27.9	0.293	0.680	-0,002	0,3
45	442	762	210	25.4	0.294	0.805		0.3
90	445	766	210	25.9	0.278	0.926		0.3

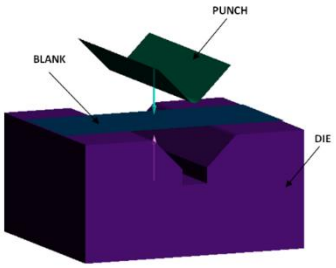

Fig. 5 CAD model of the bending tool used in the simulation

To study the effect of various configurations of constitutive models on the springback results in the FEM simulation Hill48 and Barlat89 yield criteria were used in combination with Ludwik and Swift hardening models in the numerical simulations. In this work, two isotropic hardening rules and two combined hardening rules were tested in numerical simulations. Isotropic hardening rules are defined as:

- Ludwik

$$\sigma = K \cdot \varphi^n \quad (1.)$$

- Swift

$$\sigma = K \cdot (\varphi_0 + \varphi_{pl})^n \quad (2.)$$

where σ is the true stress, K is the strength coefficient, n is the strain hardening exponent, φ0 is the pre-strain and φpl is the plastic strain. Material model constants used in both hardening rules are shown in **Table 2**.

Table 2 Material constants used for definition of hardening rules

Model	**K [MPa]**	**φ_0 [-]**	**n [-]**
Ludwik	1 330	-	0.290
Swift	1 300	0.00832	0.277

Hill yield criterion was introduced in 1948 [23, 24]. Hill proposed an anisotropic yield criterion which includes three

orthogonal symmetry planes, which is described by the following quadratic function:

$$2f(\sigma) = (G+H)\sigma_{xx}^2 + (F+H)\sigma_{yy}^2 - 2H\sigma_{xx}\sigma_{yy} + 2N\sigma_{xy}^2 \quad (3.)$$

ere σ_{xx}, $\sigma_{yy,}$ and σ_{zz} are stresses in the RD (x), TD (y), and thickness (z) directions, respectively; σ_{xy}, $\sigma_{yz,}$ and σ_{zx} are the shear stresses in xy, yz, and zx directions. Parameters F, G, H, and N are material parameters that describe the anisotropy of the material. If $F = G = H = 1$ and $N = 3$, the Hill48 function is reduced to the von Mises criterion, or as it is called in FEM code, the Hill48 isotropic criterion. A more common description is based on normal anisotropy in the 0°, 45°, and 90° directions to the rolling direction. Then the material parameters F, G, H, and N can be described by:

$$F = \frac{r_0}{r_{90}(r_0+1)}, G = \frac{1}{r_0+1}, H = \frac{r_0}{r_0+1}, \quad N = \frac{(r_0+r_{90})(1+2r_{45})}{2r_{90}(1+r_0)} \quad (4.)$$

The second yield criterion used in numerical simulations was the Barlat yield criterion. The Barlat89 model needs three parameters for its complete formulation by which it is possible to describe the plane stress behavior. The formulation is the following [25]:

$$f = a|k_1 + k_2|^M + a|k_1 - k_2|^M + (2-a)|2k_2|^M = 2\sigma_e^M \quad (5.)$$

where M is the exponent related to the crystallographic structure of the material σ_e is the initial yield stress, k_1 and k_2 can be described as:

$$k_1 = \frac{\sigma_x + h\sigma_y}{2}, k_2 = \left[\left(\frac{\sigma_x - h\sigma_y}{2}\right) + p^2\tau_{xy}^2\right]^{1/2} \quad (6.)$$

where a, h, and p are the material model parameters identified by:

$$a = \frac{2\left(\frac{\sigma_e}{\tau_{s2}}\right)^M - 2\left(1+\frac{\sigma_e}{\sigma_{90}}\right)^M}{1+\left(\frac{\sigma_e}{\sigma_{90}}\right)^M - \left(1+\frac{\sigma_e}{\sigma_{90}}\right)^M}, h = \frac{\sigma_e}{\sigma_{90}}, \quad p = \frac{\sigma_e}{\tau_{s1}}\left(\frac{2}{2a+2^M(2-a)}\right)^{\frac{1}{M}} \quad (7.)$$

where τ_{s1} and τ_{s2} are yield stresses for two different types of shear tests: $\sigma_{12} = \tau_{s1}$ for $\sigma_{11} = \sigma_{22} = 0$ and σ12 = 0 for $\sigma_{22} = -\sigma_{11} = \tau_{s2}$. The identification procedure based on the coefficients r_0 and r_{90} can be also used for the identification of parameters a and h:

$$a = 2 - 2\sqrt{\frac{r_0}{1+r_0}\cdot\frac{r_{90}}{1+r_{90}}}, h = \sqrt{\frac{r_0}{1+r_0}\cdot\frac{1+r_{90}}{r_{90}}} \quad (8.)$$

The coefficient p has to be calculated by a numerical procedure, by solving the non-linear equation or by using Equation (5.) instead. In our case, the coefficient p was achieved by solving the non-linear equation.

RESULTS AND DISCUSSION

In this section, experimental results and simulation results are presented and evaluated. Experimental results of measured springback – Arm opening angle ß after the bending process are shown in **Fig. 6**. Given the results, it can be assumed, that calibration force has a significant impact on the springback. Specimen cut direction also has an impact on the springback effect. The blanks that were cut 90° to rolling direction exhibited greater springback after bending than the blanks which were cut 0° to the rolling direction when radius R= 3 mm was used. The greater springback was measured for the sheets that were cut 0° to the rolling direction in most cases when radius R= 1 mm was tested. The assumption is that the lower value of the strain hardening component for the blanks cut 90° to rolling direction reduces the stress in the part, which has a positive impact on the springback reduction. Additionally, it can be assumed that a higher calibration force reduces springback after bending. This assumption corresponds with the numerical results. The higher strain in the bending area is a possible reason for this occurrence – springback reduction. The influence of bending radius on the springback results is mainly visible for the bending force of 1 830 N. The value of bending radius has an effect on the strain in the bending region. Thus, a smaller radius should provide a higher plastic strain rate in the bending region of the part, which has a positive impact on the springback reduction. The ratio of the total deformation at a given location to the elastic deformation is smaller and thus the springback effect is reduced.

Besides, the effects of the used yield criterion and hardening law on springback prediction were investigated. Springback results achieved using different yield criteria and hardening laws were compared with the test results and pictured in Fig. 7a and Fig 7b. From the given springback prediction results, it can be assumed, that if the higher value of calibration force is used, the lower angle ß will be measured after bending, this assumption corresponds with experimental test results. The use of different combinations of material models, yield criteria, and hardening laws showed different springback predictions, different values of arm opening angle ß. Swift's hardening law in combination with both yield criteria predicted higher values of springback after bending. Better correlation with experimental results showed the combination of Hill and Barlat yield criteria with Ludwik hardening law, but the predicted values of springback were not identical with the experimentally achieved springback values in most cases. The effect of radius on springback in numerical models is similar to the effect of radius in the experiments but less pronounced. The lower value of bending radius R=1 mm shows lower springback values compared to the higher radius value R= 3 mm.

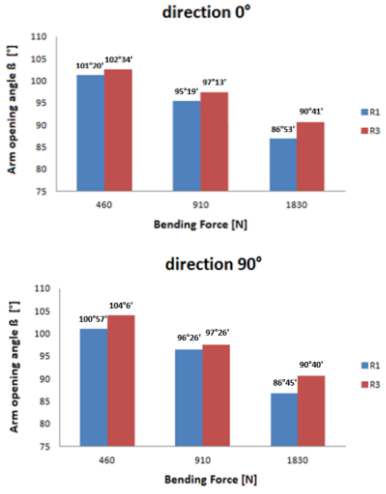

Fig. 6 Comparison of measured Arm opening angle ß [°] for both tested punch radiuses R1 and R3 used in the experiment

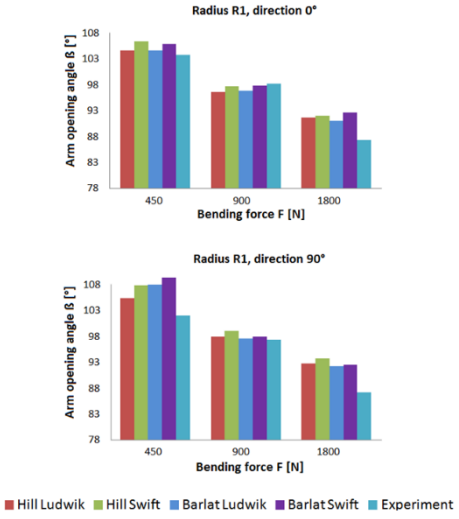

Fig. 7a Comparison of predicted Arm opening angle ß for punch radius R=1 mm

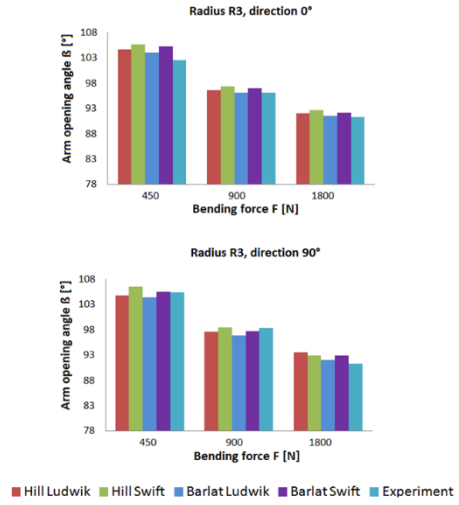

Fig. 7b Comparison of predicted Arm opening angle ß for punch radius R=3 mm

CONCLUSION

In this study, the effects of various material models in the numerical simulation on the springback prediction of TRIP steel were evaluated. The results obtained with the use of FEA, numerical simulations were compared with experimental ones. The experimental results showed the effect of direction in which sheet metal sampling was cut, bending radius and calibration force on the springback of bent TRIP steel sheet. In the numerical simulations, a combination of different yield criteria and hardening laws was tested and their impact on springback prediction was evaluated. The results showed that the best correlation between experimental and numerical results, when Hill48 and Barlat yield criteria were used in combination with Ludwik hardening law and calibration force F with the value 900 N was used. The predicted values were not the same as the experimentally achieved ones in most cases. The main reason for it can be attributed to different stress, strain values, and strain paths which depend on the material model and its inputs, which can significantly influence the springback predictions. Based on the experimental and numerical results, the following outputs can be stated:

- Calibration force has a significant impact on the springback which occurs after the forming process and it can be used as an effective tool for springback reduction.
- Specimen cut direction and bending radius affect the springback, but they have less impact on the springback compared to the calibration force.
- Hill48 and Barlat yield criteria used in combination with Ludwik hardening law showed correlation with experimental results.
- Swift hardening law in combination with both yield criteria predicted higher values of the springback in most cases.
- All of the springback predictions underestimated springback when the value of punch radius was 1 mm and the highest value of calibration force was used.
- The springback predictions were more accurate when the value of the punch radius R = 3 mm was used compared to the value of the punch radius R = 1 mm.

ACKNOWLEDGMENTS

Authors are grateful for the support of experimental works by projects APVV-17-0381, ITMS 313011T594, and VEGA 1/0384/20.

REFERENCES

1. H.L. Dai, H.J. Jiang, T. Dai, W. Xu, W.L. Luo: Journal of Alloys and Compounds, 26(708), 2017, 575–586. https://doi.org/10.1016/j.jallcom.2017.02.270.
2. T. Kvackaj, J. Bidulska, R. Bidulsky: Materials, 14(8), 2021, 1988. https://doi.org/10.3390/ma14081988.
3. H. Jirkova, K. Opatova, S. Jenicek, J. Vrtacek, L. Kucerova: Acta Metallurgica Slovaca, 25(2), 2019, 101-106. https://doi.org/10.12776/ams.v25i2.1267.
4. V. Efremenko et al.: Acta Metallurgica Slovaca, 26(3), 2020, 116-121. https://doi.org/10.36547/ams.26.3.554.
5. E. Evin, M. Tomáš: Metals, 2017, 7(7), 239. https://doi.org/10.3390/met7070239.
6. J. Majerníková, E. Spišák: Applied Mechanics and Materials, 10(474), 2014, 279-284. https://doi.org/10.4028/www.scientific.net/AMM.474.279.
7. B. Chongthairungruang, V. Uthaisangsuk: Materials and Design, 32(39), 2012, 318-328. https://doi.org/10.1016/j.matdes.2012.02.055.
8. J. Jeswiet, M. Geiger, U. Engel, M. Kleiner, M. Schikora, J. Duflou: CIRP Journal of Manufacturing Science and Technology, 13, 2008, 2-17. https://doi.org/10.1016/j.cirpj.2008.06.005.
9. K. Lawanwong, H. Hamasaki, R. Hino, F. Yoshida: The International Journal of Advanced Manufacturing Technology. 106, 2019, 1855–1867. https://dx.doi.org/10.1007/s00170-019-04678-y.
10. J. Slota, E. Spišák: Metalurgija, 47(1), 2008, 13-17.
11. J. Slota, M. Šiser, M. Dvorák: Strength of Materials, 4, 2017, 93-102. https://doi.org/10.1007/s11223-017-9900-6.
12. T. Yoshida, K. Sato, E. Isogai, K. Hashimoto: Springback problems in forming of High-Strength steel sheets and countermeasures. Nippon steel technical report, 103, 2013, 4-10.

13. M. Samuel: Journal of material processing technology, 105, 2013, 382-393. https://doi.org/10.1016/S0924-0136(00)00587-2.
14. P. Mulidrán, E. Spišák, M. Tomáš, J. Slota, J. Majerníková: Metals, 10(9), 2020, 1119. https://doi.org/10.3390/met10091119.
15. P. Mulidrán, M. Šiser, J. Slota, E. Spišák, T. Sleziak: Metals, 8(6), 2018, 435. https://doi.org/10.3390/met8060435.
16. D. Neto, M. Oliveira, A.D. Santos, J. Alves, L.F. Menezes: International Journal of Mechanical Sciences, 122, 2017, 244–254. https://doi.org/10.1016/j.ijmecsci.2017.01.037.
17. J. Slota, M. Jurčišin, L. Lăzărescu: Acta Metallurgica Slovaca, 20, 2014, 236–243. https://doi.org/10.12776/ams.v20i2.287.
18. K. Seo, J. Kim, H. Lee, J.H. Kim, B. Kim: Metals, 18 (8), 2017. https://doi.org/10.4271/2002-01-0159.
19. W.A.B. Baara, B. Baharudin, M. Ariffin, M. Ismail: Metals, 9, 2019, 511. https://doi.org/10.3390/met9050511.
20. X. Cui, A. Xiao, Z. Du, Z. Yan, H. Yu: Metals, 10, 2020, 390. https://doi.org/10.3390/met10030390.
21. P. Mulidrán, E. Spišák, M. Tomáš, V. Rohaľ, F. Stachowicz: Acta Mechanica Slovaca, 23 (4), 2019, 14-18. https://doi.org/10.21496/ams.2019.022.
22. E. Evin, M. Tomáš: Acta Metallurgica Slovaca, 25 (4), 2019, 208-216. https://doi.org/10.12776/ams.v25i4.1362.
23. R. Hill: Proceedings of the royal society A. 1948, 193, 281–297.
24. S. Bruschi, T. Altan, D. Banabic, P. Bariani, A. Brosius, J. Cao, A. Ghiotti, M. Khraisheh, M. Merklein: CIRP Annals, 63, 2014, 727–749. https://doi.org/10.1016/j.cirp.2014.05.005.
25. F. Barlat, J. Brem, J.W. Yoon, K. Chung, R. Dick, D. Lege: International Journal of Plasticity, 19, 2003, 1297–1319. https://doi.org/10.1016/S0749-6419(02)00019-0.